Local Vote Decision Fusion for Target Detection in Wireless Sensor Networks

Natallia Katenka, *Elizaveta Levina, and George Michailidis

***Abstract*— This paper examines the problem of target detection by a wireless sensor network. Sensors acquire measurements emitted from the target that are corrupted by noise, and initially make individual decisions about the presence/absence of the target. We propose the Local Vote Decision Fusion algorithm, in which sensors first correct their decisions using decisions of neighboring sensors, and then make a collective decision as a network. An explicit formula that approximates the system's decision threshold for a given false alarm rate is derived using limit theorems for random fields, which provides a theoretical performance guarantee for the algorithm. We examine both distance- and nearest neighbor-based versions of the local vote algorithm for grid and random sensor deployments and show that, for a fixed system false alarm, the local vote correction achieves significantly higher target detection rate than decision fusion based on uncorrected decisions. The algorithm does not depend on the signal model and is shown to be robust to different types of signal decay. We also extend this framework to temporal fusion, where information becomes available over time.**

Keywords: sensor network, target detection, threshold rule, decision fusion, temporal decisions.

EDICS: SEN-FUSE

I. Introduction and Problem Formulation

Wireless sensor networks are widely used for monitoring natural phenomena in space and over time, as well as for target detection and tracking [1]. In general, sensor networks are built from small, inexpensive devices that have short-range sensing capabilities and limited computational and communication capacity. Cooperation among sensors enhances their target detection potential, especially if the individual sensors are only capable of providing single bit (binary) results; namely, whether a target is present or not within their sensing range. Typically each sensor obtains an energy reading from the environment, which could be temperature, acoustic signal, vibration, etc. There has been a substantial amount of work on data fusion for target detection, where the question is how to efficiently integrate the available information from the individual sensors, in order for the network to reach a decision about the presence of a target over a monitoring region.

Suppose that N sensors have been deployed at locations $s_i,\ i = 1, \ldots, N$, over a two-dimensional monitoring region R, which without loss of generality corresponds to the unit square. A target at location $v \in R$ emits a signal captured by the sensors. Let $E_i = S_i + \epsilon_i$ denote the energy measured by the i-th sensor, where $S_i \equiv S_i(v)$ is the signal from the target measured at location i, and ϵ_i, $i = 1 \ldots N$ is i.i.d. random noise. Based on the observed energy levels E_i, each sensor reaches a decision $d_i \in \{0, 1\}$ regarding the presence of the target in the monitoring area. The decision depends on whether the energy level exceeds a pre-specified threshold τ_i, which determines the individual sensor's false alarm probability; i.e., $d_i = I(E_i \geq \tau_i)$, where $I(\cdot)$ is the indicator function.

The two main options for reaching a joint decision are *value fusion*, where sensors transmit the energy readings back to the fusion center, and *decision fusion*, where each sensor decides first whether a target is present and only the binary decisions are transmitted. In [2] value and decision fusion were compared and it was found that the former performs better in terms of detection probability for low noise levels; however, for noisy energy measurements decision fusion proves more robust. Further, it offers significant savings in communications costs, since only *positive* one-bit decisions need to be transmitted. For these reasons, in this paper we focus on decision fusion.

The classical approach to this problem (see [3] for a comprehensive review) is to assume a specific model for the signal and frame it as a hypothesis test of the null hypothesis H_0: no target is present vs. the alternative H_1: there is a target in the field. This approach was used by fusion algorithms developed in the 1980's with applications to surveillance systems (e.g. radars). Optimal decision rules based on classical Bayesian decision theory have been worked out when both the signal and noise distributions are known, for independent [4], [5] and correlated [6] decisions, though in the latter case the computations are cumbersome. In [4], it is assumed that the false alarm and detection probabilities are the same for all sensors, a fairly reasonable assumption for a remote target in, say, a missile defense system, but not for a wireless sensor network with a relatively small target in the middle of a large region. In [5], optimal weights (in the sense of classical decision theory) were derived for combining decisions d_i if the detection and false alarm probabilities are known for all sensors. The corresponding Chair-Varshney fusion rule is optimal in such a setting. Another way to derive an optimal rule is to apply the local asymptotic normality framework [7]. However, for a wireless sensor network, the assumption of known detection probabilities is unrealistic [8]: even if a specific model for the signal is assumed and all model parameters are known, the detection probability for each

The authors are with the Department of Statistics, The University of Michigan, 1085 South University, Ann Arbor, MI 48109. Telephone: (734) 763–3519, Fax: (734) 763–4676. Email: {nkatenka, elevina, gmichail}@umich.edu

The authors would like to thank the AE Lang Tong and three anonymous referees for many useful comments and suggestions. They would also like to thank M.D. Penrose for pointing out recent results on limit theorems for random graphs.

sensor depends on its distance from the target, and assuming a known location for the target would defeat the whole purpose of target detection. Further, the assumption of a known signal model can also be restrictive, since there may be different types of targets present, whose signals follow different models.

In this paper, we propose a different approach to decision fusion: we make no assumptions about the signal model whatsoever (other than that the signal is positive). The null hypothesis of no target present is H_0: $S_i = 0$ for all i, while the alternative is simply H_1: $S_i > 0$ for some i. This approach is unlikely to be optimal if a specific signal model is known in advance, since a better performance can be achieved under additional assumptions; however, it has the advantage that it is applicable even when no prior knowledge about the target's signal characteristics is available, as empirically shown in Section III. Note that this formulation follows the classical (frequentist) approach of treating the S_i's as unknown non-random parameters. Then, the energy readings E_i and the corresponding decisions d_i are independent, since the only randomness comes from the i.i.d. noise ϵ_i. Further, we assume that all sensors are identical, and that they all use the same threshold $\tau_i = \tau$. Then under H_0, all E_i's are i.i.d. and all sensors have the same false alarm probability $\alpha = P_{H_0}(d_i = 1)$. In contrast, a large body of literature adopts the so-called *conditional independence* assumption: $P(E_1, \ldots, E_N|H_m) = \prod_{i=1}^{N} P(E_i|H_m)$ for $m = 0, 1$. This assumption is inherently Bayesian, since conditioning on the hypothesis implies that the signal means S_i's are treated as random variables.

A consequence of not assuming any particular model for the signal is that the optimal Chair-Varshney type weighted rules can not be computed. Nevertheless, the following simple model-independent decision fusion algorithm studied in the literature (e.g. [2]) can be used as a benchmark comparison. We will refer to it as *ordinary decision fusion* (ODF):

Ordinary Decision Fusion:

1) Each sensor i makes its own decision $d_i \in \{0, 1\}$ w.r.t. the sensor threshold τ, $d_i = I(E_i \geq \tau)$;
2) Sensors transmit positive decisions to the fusion center;
3) The fusion center obtains final decision based on a pre-specified threshold T, $I(\sum_i d_i \geq T)$.

In the remainder of the paper, it is assumed that communication and networking issues, such as knowledge about locations of the sensors, a lossless communication protocol, synchronized transmissions to other sensors and the fusion center, wireless sensor connectivity issues, etc., have been settled in advance and we focus only on the collaborative signal processing task at hand. An integrated approach of decision fusion over lossy channels is discussed in [9].

Given a target in R, the objective of the sensor network is to maximize its probability of detection D, while controlling the corresponding system-wide false alarm probability F. The more recent work on decision fusion for target detection by wireless sensor networks has primarily focused on threshold selection, both for individual sensors and the global decision. We note that, for any given sensor false alarm probability α, the global threshold T can always be selected to achieve the desired overall system false alarm F; hence, in our problem formulation it is not possible to optimize both thresholds simultaneously. Under the assumption of independent sensor decisions, expressions for the false alarm and detection probabilities have been either calculated exactly using binomial probabilities [10], or approximated using the central limit theorem [11] and the saddle-point approximation [12], or bounded using Chebyshev's inequality [13]. These calculations typically assume known sensor detection rates, which is unrealistic for a target in an unknown location. The expressions for the false alarm probability can be used to set the threshold, but none of these techniques would work for our proposed algorithm, since they rely on independence of sensor decisions.

On the algorithmic side, alternatives to ordinary decision fusion have been proposed. Distance Weighted Voting [14] weighs individual sensor decisions by the inverse of their distance to the target, which applies only to detection at a pre-specified location. Confidence Weighted Voting [15], perhaps closest in spirit to what we propose, weighs sensor decisions by a measure of confidence based on the neighborhood agreement. Finally, in [16] the decision for a pre-specified location is made by majority vote in its neighborhood, but this was only derived for a 3-sensor system. No analytical performance guarantees exist for these methods, and it is not clear how to choose thresholds to achieve a desired false alarm rate.

This paper makes the following two contributions: first, a new decision fusion algorithm based on first locally adjusting individual sensors' decisions and subsequently integrating them at the network level is proposed. Second, we provide a rigorously derived analytical approximation for the system-wide decision threshold level T as a function of the system-wide false alarm probability F, obtained using limit theorems for random fields. This ensures that one can design a network with a guaranteed false alarm rate using our algorithm. We show that the approximation performs very satisfactorily for both random and fixed grid deployments, even for networks comprised of a small number of sensors. Further, the proposed decision fusion algorithm substantially outperforms ordinary decision fusion in terms of target detection probability for the majority of the scenarios examined, and achieves good results at a significantly lower signal-to-noise ratio. Finally, we present how to extend this algorithm to temporal decision fusion, which allows detection of moving targets over time.

II. Decision Fusion: Algorithms and Analysis

In order to guarantee the overall system performance of decision fusion for target detection, one must be able to obtain the threshold T for the whole network, given an individual sensor's and the system's false alarm probabilities α and F, respectively. It is assumed that α is determined either by hardware specifications or from information about background noise levels, whereas F is selected by the network's operator.

We start our exposition from the ordinary decision fusion algorithm, where the sensors' decisions are simply added at the fusion center, and give an expression for the false alarm rate and the corresponding target detection probability (similar analysis can be found e.g. in [10], [17]). Let G denote the distribution function of the noise levels, i.e. $\epsilon_i \sim G$, and let

$\alpha = 1 - G(\tau)$. In the absence of a target, the probability of a positive decision (false alarm probability) is given by the right tail of the binomial distribution,

$$F = P(\sum_{i=1}^{N} d_i \geq T) = \sum_{i=T}^{N} \binom{N}{i} \alpha^i (1-\alpha)^{N-i}, \quad (1)$$

since sensors make individual decisions independently.

In the presence of a large number of sensors, the above tail probability can be fairly accurately determined by the normal approximation given by

$$F \approx 1 - \Phi\left(\frac{T - N\alpha}{\sqrt{N\alpha(1-\alpha)}}\right), \quad (2)$$

where $\Phi(\cdot)$ denotes the standard normal cumulative distribution function. Therefore, for specific sensor and system false alarm probabilities α and F, one can compute the corresponding threshold T. Note that knowledge of the background noise distribution G is not required, as long as α is known. Then, a target is detected by the network if at least T sensors measure energy levels that exceed their individual threshold τ. Hence, the probability of detection is given by

$$D = \sum_{i=T}^{N} \sum_{\pi \in \Gamma} \prod_{j=1}^{i} \left(1 - G(\tau - S_{\pi(j)})\right) \prod_{j=i+1}^{N} G(\tau - S_{\pi(j)}), \quad (3)$$

where Γ denotes the set of all permutations of $\{1, \ldots, N\}$. The first product term corresponds to the probability that sensors $\pi(1), \ldots, \pi(i)$ make positive decisions, while the second product term corresponds to the probability that sensors $\pi(i+1), \ldots, \pi(N)$ make negative decisions. The detection probability depends on the target's and the sensors' locations, signal parameters, and the noise distribution. Even though in principle (3) gives a closed-form analytical expression for detection probability, computing it this way is not feasible numerically; instead, we compute it through simulation (see Section III).

A. Local Vote Decision Fusion: the algorithm

We propose next a modification of the ODF mechanism that first adjusts each sensor's decision locally by taking a majority vote in its neighborhood. For each sensor i, the neighborhood $U(i)$ can be defined as either all sensors within a fixed distance r (e.g., communications range), or as a fixed number of its nearest neighbors. By definition, $i \in U(i)$, so the sensor's own decision is always taken into account.

Local Vote Decision Fusion (LVDF):

1) Sensor i makes an *initial* decision d_i independent of all other sensors and communicates it to all other sensors j in its neighborhood $U(i)$,
2) Subsequently, given a set of decisions $\{d_j : j \in U(i)\}$, sensor i adjusts its initial decision according to a majority vote; i.e., $Z_i = I(\sum_{j \in U(i)} d_j > M_i/2)$, where $M_i = |U(i)|$ denotes the size of the neighborhood.
3) The positive updated decisions Z_i are communicated to the fusion center, which makes the final decision $I(\sum_{i=1}^{N} Z_i \geq T_\ell)$.

In practice, sensors only need to communicate positive decisions in step 1; an absence of communication according to some pre-specified protocol implies that $d_i = 0$. In Figure

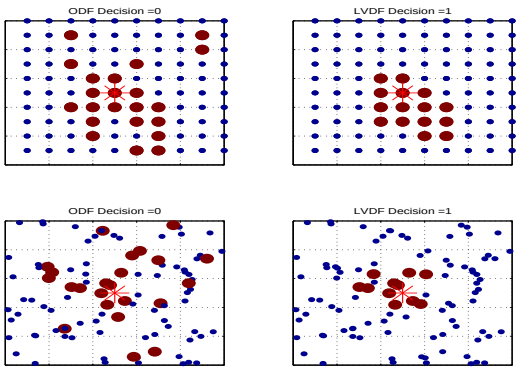

Fig. 1. Ordinary vs Local Vote decision fusion under a square grid design (top panels) and random deployment (bottom panels). The network is comprised of 100 sensors, with individual sensor false alarm probability $\alpha = 0.2$, system-wide false alarm probability $F = 0.1$ and a target located at the center of the monitored region R. The signal is generated by the model $S_i = S_0 \exp(-||s_i - v||^2/\eta^2)$, with $S_0 = 2$, $\eta = 0.1$, and the measured energy is corrupted by Gaussian noise with $\sigma = 0.4$.

1, the advantage of local vote decision fusion over ordinary decision fusion is illustrated for both random and fixed grid deployments. Under ordinary decision fusion, the threshold T is higher since more wrong decisions from sensors located far away from the target are expected; these false positives have a significant adverse effect on the sensor network's final decision. On the other hand, the proposed local vote mechanism fixes those isolated decisions and helps the network reach the correct conclusion. If communications to neighbors are cheaper than those to the fusion center, which is typical, LVDF also reduces the overall communication costs since by canceling out false positives it reduces the number of positive decisions which need to be communicated to the fusion center.

B. Local Vote Decision Fusion: threshold selection

We derive next the system-wide threshold value T_ℓ for LVDF that guarantees a false alarm probability F. The strategy is to derive a normal approximation for F for large sensor networks. However, unlike the initial decisions, the updated ones exhibit dependences, a fact that introduces certain technical challenges that are resolved next.

We start by calculating the expected value μ_i and variance σ_i^2 of the updated decision Z_i under H_0:

$$\mu_i = P(Z_i = 1) = \sum_{j=[M_i/2]+1}^{M_i} \binom{M_i}{j} \alpha^j (1-\alpha)^{M_i - j}, \quad (4)$$

where $[x]$ denotes the largest integer smaller than or equal to x. The variance is given by $\sigma_i^2 = \mu_i(1-\mu_i)$.

The dependence between Z_i and Z_j, $j \neq i$ comes from the intersection of their respective neighborhoods $U(i)$ and $U(j)$. Let n_{ij} denote the number of sensors in the intersection $U(i) \cap U(j)$. In order to calculate the covariance between Z_i

and Z_j we first compute $E(Z_iZ_j) = P(Z_i = Z_j = 1)$. Let A be the number of positive decisions in $U(i) \cap U(j)$, B the number of positive decisions in $U(i)$ but not in $U(j)$, and C the number of positive decisions in $U(j)$ but not in $U(i)$, and note that A, B, and C are independent. Then we can write (letting $\binom{a}{b} \equiv 0$ if $b < 0$)

$$E(Z_iZ_j) = \sum_{k=0}^{n_{ij}} P(A = k)\, P(B > \frac{M_i}{2} - k)\, P(C > \frac{M_j}{2} - k), \quad (5)$$

where

$$\begin{aligned} P(A = k) &= \binom{n_{ij}}{k} \alpha^k (1-\alpha)^{n_{ij}-k}, \\ P(B > \frac{M_i}{2} - k) &= \sum_{q=[\frac{M_i}{2}]-k+1}^{M_i - n_{ij}} \binom{M_i - n_{ij}}{q} \alpha^q (1-\alpha)^{M_i - n_{ij} - q}, \\ P(C > \frac{M_j}{2} - k) &= \sum_{q=[\frac{M_j}{2}]-k+1}^{M_j - n_{ij}} \binom{M_j - n_{ij}}{q} \alpha^q (1-\alpha)^{M_j - n_{ij} - q}. \end{aligned}$$

The covariance is then given by

$$\text{Cov}(Z_i, Z_j) = [E(Z_iZ_j) - \mu_i\mu_j] I(n_{ij} > 0). \quad (6)$$

Under the assumption that the target is absent, the system's false alarm probability is given by

$$F = P\left(\sum_{i=1}^{N} Z_i \geq T_\ell \right), \quad (7)$$

where T_ℓ denotes the local-vote decision fusion threshold. The updated decisions $\{Z_i;\ i = 1, \ldots, N\}$ form a dependent random field. The central limit theorem applies to the $\sum Z_i$ (see Appendix), both for sensors deployed on a regular grid or at random. The following approximation then holds:

$$F \approx 1 - \Phi\left(\frac{T_l - \sum_{i=1}^{N} \mu_i}{\sqrt{\sum_{i=1}^{N} \sigma_i^2 + \sum_{i \neq j, n_{ij} > 0} \text{Cov}(Z_i, Z_j)}} \right). \quad (8)$$

Remark 1: Fixed neighborhood size

In some settings (e.g., dense deployments or regular grids) the number of neighbors may be fixed to a pre-specified number with $|U(i)| = M$ for all i. In this case we have $Z_i = I\left\{ \sum_{j \in U(i)} d_j > \frac{M}{2} \right\}$, which shows that the Z_i's are dependent but now *identically* distributed. Hence, the mean $E(Z_i) = \mu$ and the variance $\text{Var}(Z_i) = \sigma^2$ can be calculated using (4). Then, $E(Z_iZ_j)$ can be calculated from (5) with $M_i = M_j = M$ and the resulting covariance is given by $\text{Cov}(Z_i, Z_j) = [E(Z_iZ_j) - \mu^2] I(n_{ij} > 0)$. The normal approximation simplifies accordingly.

Remark 2: Regular Grids

In some applications, it may be possible to deploy the sensors along a regular grid. In this case the false alarm approximation (8) further simplifies under the assumption that each sensor has exactly M neighbors to consult including itself (ignoring edge effects). In practice, this can be achieved by ignoring corrected decisions of sensors on the edges, effectively reducing the grid size. On a regular grid, the one-hop neighborhood contains either $M = 5$ (diamond-shaped neighborhood) or 9 neighbors (square neighborhood), depending on whether diagonally located nearest neighbors are included or not.

(i) Square neighborhood: The number of hops (layers) away from the sensor at the center determines the size of the neighborhood. Let m denote the number of layers considered. Then, the size of the neighborhood $U(i)$ is given by $M = (2m+1)^2$ everywhere except at the edges, and in general by $M_i = m_i^L \times m_i^W$, where m_i^L and m_i^W are the length and the width of $U(i)$. Let $t = (t_1, t_2)$ be a location shift and $U(i+t)$ the neighborhood of the sensor located at $s_i + t$. Then the size of a non-empty intersection of $U(i)$ and $U(i+t)$ is given by $n_{i,i+t} = (\max(m_i^L, m_{i+t}^L) - |t_1|)(\max(m_i^W, m_{i+t}^W) - |t_2|)$. The covariance is given by $\text{Cov}(Z_i, Z_{i+t}) = [E(Z_iZ_{i+t}) - \mu_i\mu_{i+t}] I(n_{i,i+t} > 0)$ and the normal approximation of F can be obtained as before.

(ii) Diamond-shaped neighborhood: We only consider the single-layer neighborhood with $M = 5$. The possible values for the size of non-empty intersections of $U(i)$ and $U(j)$ are

$$n_{ij} = |U(i) \cap U(j)| = \begin{cases} 1, & \|s_i - s_j\| = 2h \\ 2, & h \leq \|s_i - s_j\| \leq h\sqrt{2} \end{cases} \quad (9)$$

where $2h$ is the length of the diamond's diagonal. The approximation for F can then be straightforwardly obtained.

III. Performance Evaluation

In this section we evaluate the proposed local vote decision fusion scheme. The models used to generate signals are:

$$\text{M1: } S_i = S_0 \exp(-\frac{||s_i - v||^2}{\eta^2}), \ \text{M2: } S_i = \frac{S_0}{1 + (||s_i - v||/\eta)^3}, \quad (10)$$

while measured energies are contaminated by Gaussian noise with mean zero and variance σ^2. The main difference between the two models is that under M1 the signal decays exponentially fast, while under M2, polynomially fast. Notice that the parameter η scales the attenuation of the signal within the monitored region R and essentially determines the effective size of the target. These models capture the characteristics of physical processes. For example, M1 with its exponential rate is most appropriate for temperature signals, due to Newton's law of cooling. On the other hand, M2 has been used in the literature as a model for acoustic signals, with the exponent in the denominator ranging between 2 and 5 [18], [19]. Finally, for ease of interpretation in simulations, we give the values of the baseline signal strength S_0 and the signal-to-noise ratio expressed in dB units, given by SNR=$10 \log_{10}(S_0/\sigma)$.

Quality of the approximation: We start by examining the quality of the normal approximation of the network's false alarm probability. The left panel of Figure 2 shows the approximation error for regular n by n grid designs, for $M = 9$ and $M = 5$ size neighborhoods for LVDF, together with ODF, which corresponds to $M = 1$. The true values of false alarm are based on 3,000 simulations of noise, with Monte Carlo error present in the 4th significant digit. The approximation for ODF is simply the normal approximation to the binomial distribution, and thus is the most accurate. As M increases, the dependencies among the decisions become stronger, and the quality of the approximation deteriorates. On the other hand, as

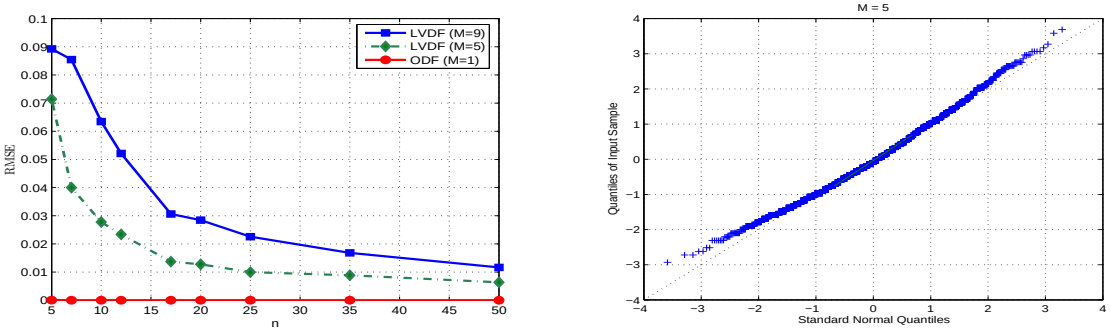

Fig. 2. Left panel: Root mean squared error (RMSE) of the normal approximation of the system's false alarm probability for grids with neighborhood sizes $M = 5,\ 9$, together with ODF, as a function of the grid size n (number of sensors $N = n^2$). The individual sensor's false alarm $\alpha = 0.2$, and the RMSE is computed over the range of $F = 0 \ldots 0.5$. Right panel: A plot of the calculated false alarm probability quantiles against the theoretical ones of a standard normal distribution for a 25×25 grid, with $\alpha = 0.2$ and $M = 5$.

the size n of the grid increases, the approximation improves. Nevertheless, the quality of the approximation remains very good even for moderate network sizes. A quantile-quantile plot of the calculated false alarm probability obtained from 3,000 simulations vs. those from a standard normal distribution for a 25×25 grid, with $\alpha = 0.2$ and the neighborhood size $M = 5$, is shown in the right panel of Figure 2. It can be seen that the approximation is very good, with only a slight departure from normality in the tails.

We examine next the quality of the approximation for random deployments for two variants of LVDF (Table I). The first one is *distance based* (D-LVDF), which defines the neighborhood $U(i)$ as all sensors within a circle of fixed radius r from sensor i, i.e., $U(i) = \{j : ||s_i - s_j|| \leq r\}$. The second one based on *nearest neighbors* (NN-LVDF) fixes the number of neighbors to be considered; i.e., $U(i) = \{i\} \cup \{$M-1 nearest neighbors of $i\}$. In order to make the two methods comparable, for D-LVDF we set M to be the average number of points in a circle of radius r; hence, $M = N(\pi r^2)$ and $r = \sqrt{M/(N\pi)}$.

Columns A1 and A2 in Table I give the RMSE of the general approximation formula (8) for D-LVDF and NN-LVDF, averaged over 100 random deployments (Monte Carlo error is in the 4th digit). The true false alarms for each deployment are obtained from 3000 noise simulations. The settings used are $M = 5$, $r = \sqrt{M/(N\pi)}$ for the size of the NN- and D-LVDF neighborhoods, $\alpha = 0.2$; the RMSE is computed over the range $F = 0 \ldots 0.5$. As expected, the quality of the approximation improves for larger network sizes $N = n^2$, but the approximation is reasonable even for smaller networks.

The general approximation (8) depends on sensor locations, which we assume are known or can be obtained through a localization algorithm. However, examination of the approximation (8) shows that it depends on sensor locations only through the *distribution* of neighborhood sizes M_i and their intersections n_{ij}; and, while the actual locations will change from deployment to deployment, the distribution of neighborhood sizes does not change much. Columns B1 and B2 in Table I show approximation errors obtained by computing the threshold (8) from a *single* arbitrary random deployment and then averaging the errors over 100 different random deployments; it can be seen that the differences are very small and therefore localization can be avoided in practice.

	D - LVDF			NN - LVDF		
n	A1	B1	C1	A2	B2	C2
10	0.023	0.026	0.099	0.025	0.025	0.026
25	0.009	0.019	0.260	0.014	0.014	0.015
50	0.006	0.016	0.443	0.011	0.011	0.011

TABLE I

RMSE FOR RANDOM DEPLOYMENTS WITH $M = 5$. A: APPROXIMATION (8); B: APPROXIMATION (8) BASED ON A SINGLE FIXED DEPLOYMENT; C: APPROXIMATION FOR A $M = 5$ SIZE NEIGHBORHOOD ON A REGULAR GRID (MONTE CARLO ERROR PRESENT IN THE 4TH DIGIT).

An even greater simplification would be to approximate the random deployment with a fixed grid. Columns C1 and C2 in Table I show that this approximation is reasonable for NN-LVDF but not D-LVDF. This is expected, since the distributions of neighborhood sizes are very similar for the grid and NN-LVDF (all $M_i = M$, so only the intersections vary), but not at all similar for D-LVDF and the grid.

Target detection probability: The main performance metric for LVDF is the probability of target detection D, which we examine here for a target located at the center of region R and a network comprised of 100 sensors. We compare ODF and LVDF using a neighborhood size $M = 9$ under random and square grid deployments. The differences between D-LVDF and NN-LVDF are fairly negligible and therefore only the detection probability for D-LVDF is shown and referred to as LVDF. The plots are based on averages from 1000 simulations.

There are four main parameters that influence D and which are examined in the simulation study: system false alarm probability F (the ROC curve, Fig. 3), SNR (Fig. 4), sensor's false alarm probability α (Fig. 5), and signal decay parameter η (Fig. 6). The models M1 and M2 provide a comparison between a localized (M1) and a more diffuse signal (M2). The main conclusions reached by studying these plots are summarized next:

– The LVDF algorithm almost uniformly outperforms the ODF one. The only exception is for very low values of α, since in

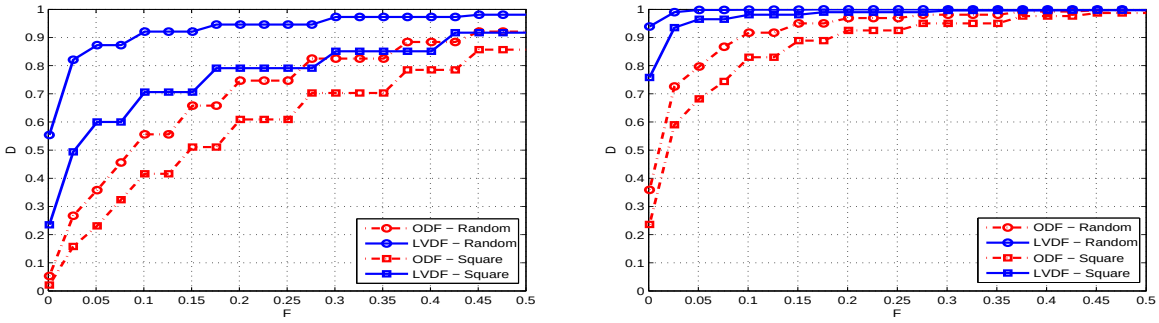

Fig. 3. Probability of detection as a function of the system-wide false alarm probability F (ROC curve) for models M1 (left panel) and M2 (right panel) with $\alpha = 0.2$, $SNR = 7$, $\eta = 0.1$.

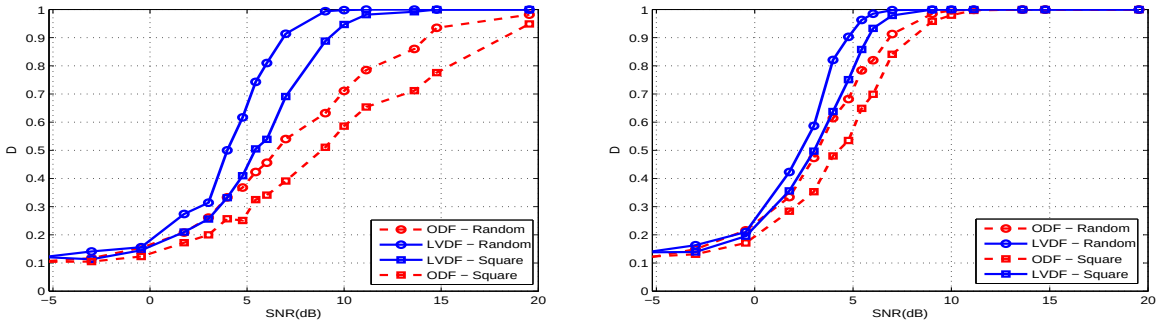

Fig. 4. Probability of target detection as a function of SNR (in dB) for models M1 (left panel) and M2 (right panel) with $\alpha = 0.2$, $F = 0.1$, $\eta = 0.1$.

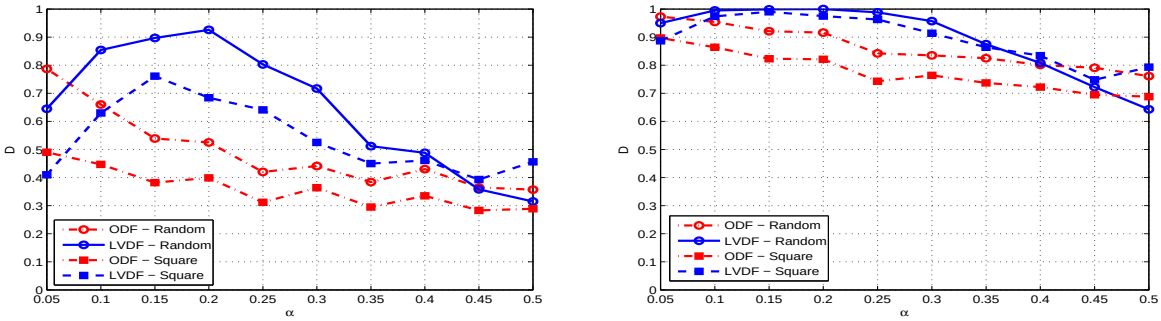

Fig. 5. Probability of target detection as a function of the false alarm for a single sensor α for models M1 (left panel) and M2 (right panel) with $F = 0.1$, $SNR = 7$, $\eta = 0.1$.

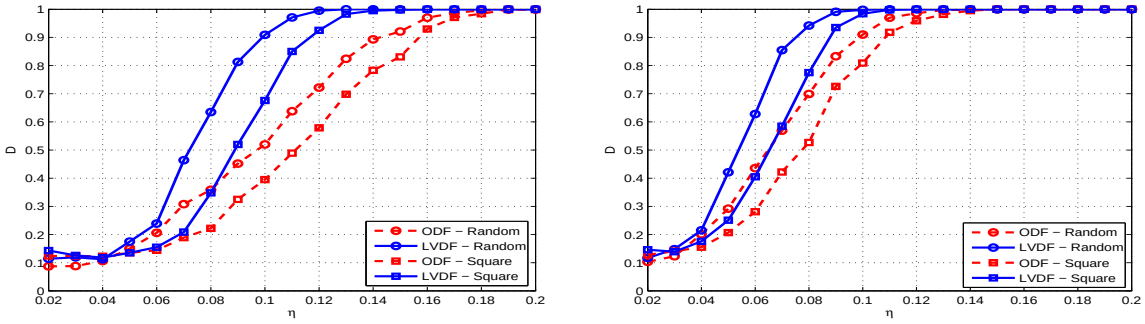

Fig. 6. Probability of target detection as a function of the signal decay parameter η for models M1 (left panel) and M2 (right panel) with $\alpha = 0.2$, $F = 0.1$, $SNR = 7$.

the absence of any false positives, it can not help denoising the decisions.
– LVDF can have very substantial gains -up to a two-fold increase- in detection probabilities. The largest gains occur for more localized signals (M1), and for moderate values of α's and η.
– Detection probabilities for both ODF and LVDF are lower for the M1 model compared to the M2 one; this is expected in view of the polynomial decay of tails under M2. However, the corresponding gains from LVDF are larger for the M1 model.
– For very low values of η (a very small target), or SNR, neither method can detect the target and the probability decreases to the system false alarm F. Conversely, for very large targets or very high SNR values, both methods achieve near-perfect detection.
– Both LVDF and ODF exhibit a superior performance under random deployments. This is due to the discretization of the grid – our isotropic signal models generate a circular target, which is covered by fewer sensors from a square grid than from a random deployment. The differences become negligible for denser networks ($N \geq 400$ – results not shown here).

Energy Savings: The exact amount of energy savings will depend on the system set-up and the cost of in-network transmissions relative to transmissions to fusion center. However, since LVDF leads to better detection regardless of whether it can provide energy savings, it can be performed at the fusion center after the original decisions are transmitted. If transmissions to fusion center are more expensive, then the energy savings potential of LVDF over ODF can be assessed from the number of positive decisions transmitted to the fusion center. These are shown in Fig. 7 for both algorithms as a function of α and η for model M1 (the pattern for M2 is very similar).

System design: We examine next the sensitivity of the target detection probability to the size of the local vote neighborhood, since this parameter can impact the operational characteristics of the sensor network. The setting is as follows: individual false alarm probability is fixed at $\alpha = 0.2$, system false alarm is $F = 0.1$, and the signal is generated by model M1 with $S_0 = 2$, SNR=7 and $\eta \in \{0.05, 0.10, 0.15\}$. In Figure 8, the probability of target detection D as a function of M is shown for these three levels of the signal decay parameter η. It can be seen that when the signal is highly localized ($\eta = 0.05$) the detection probability does not exceed 0.5 and is maximized for small values of M, whereas when the signal diffuses across R, the detection probability is almost 1 for almost all values of M examined. For $\eta = 0.1$, the optimal neighborhood size is around 10, and the drop in D for larger values of M occurs when the size of the neighborhood becomes larger than the target. In this case, only a few sensors in the neighborhood pick up the signal and thus the majority vote tends to indicate the target is absent. A similar pattern occurs for model M2. These plots indicate that when designing a wireless sensor network employing a LVDF mechanism, one should choose the size of the neighborhood comparable to the size of the smallest target one is interested in detecting, since large targets will be easy to spot.

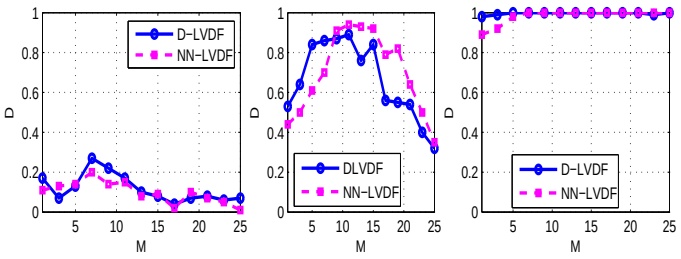

Fig. 8. Target detection probability for various levels of signal decay: left panel: $\eta = 0.05$, middle panel: $\eta = 0.10$, right panel: $\eta = 0.15$.

IV. Temporal Decision Fusion

In previous sections, the problem of decision fusion for target detection by a sensor network has been studied when only one set of energy measurements is available. However, target detection is often performed continuously over time, as the sensor network collects information and updates its decisions. We examine next the problem of temporal decision fusion. We assume that at every time slot $t = 0, 1, 2, \ldots$ the sensors obtain energy measurements and make decisions, and extend the proposed local vote decision fusion framework to decisions made over time.

Denote by Z_i^t the decision of sensor i at time t corrected according to the proposed LVDF scheme. The values Z_i^t are stored and processed by the fusion center. We propose combining decisions over time with an exponentially weighted moving average (EWMA) with parameter λ, $0 \leq \lambda \leq 1$: for all $i = 1, \ldots, N$, let $Y_i^0 = Z_i^0$ and

$$Y_i^t = \lambda Z_i^t + (1-\lambda) Y_i^{t-1}, \ t = 1, 2, \ldots \tag{11}$$

The parameter λ determines how much weight to give to the present vs. the past: in slowly changing environments or for slowly moving targets smaller λ will be better, and vice versa. The decision of the network at time t is given by $\tilde{D}_t = I\left(\sum_{i=1}^N Y_i^t \geq \tilde{T}_\ell\right)$. As before, the goal becomes to obtain an approximation for the system-wide false alarm probability that allows us to calculate $\tilde{T}_\ell$. We examine the case where the energy measurements E_i and consequently the corrected decisions Z_i^t are independent over time; the case where the Z_i^ts are correlated over time, due to correlated noise in the energy measurements, is studied through simulation in Section IV-A.

Straightforward algebra shows that, for all $i, j = 1 \ldots N$, and all $t = 1, 2, \ldots$, $E(Y_i^t) = E(Z_i^t) = \mu_i$, and

$$\text{Cov}(Y_i^t, Y_j^t) = \lambda^2 \text{Cov}(Z_i^t, Z_j^t) + (1-\lambda)^2 \text{Cov}(Y_i^{t-1}, Y_j^{t-1}). \tag{12}$$

Iterating the recursive covariance formula (12) we obtain

$$\text{Cov}(Y_i^t, Y_j^t) = ((1-\lambda)^{2t} + \lambda^2 \sum_{k=0}^{t-1} (1-\lambda)^{2k}) \text{Cov}(Z_i^k, Z_j^k), \tag{13}$$

and letting $t \to \infty$ we finally get, for large t,

$$\text{Cov}(Y_i^t, Y_j^t) = \frac{\lambda}{2-\lambda} \text{Cov}(Z_i^0, Z_j^0). \tag{14}$$

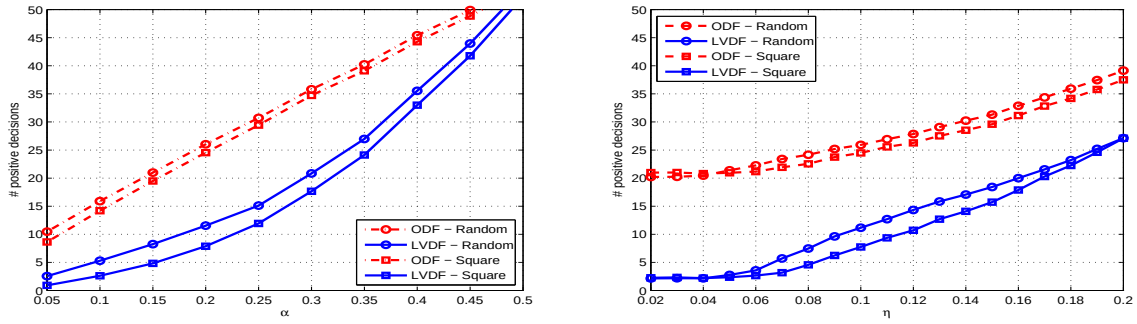

Fig. 7. Number of positive decisions as a function of the sensor's false alarm α (left panel, with $\eta = 0.1$) and as a function of the signal decay parameter η (right panel, with $\alpha = 0.2$) for model M1 with $F = 0.1$ and $SNR = 7$.

The geometric series converge very quickly for reasonable values of λ, at the rate $\mathcal{O}(1-\lambda)^{2t}$. The approximation formula for the system-wide false alarm probability F is given by

$$F \approx 1 - \Phi\left(\frac{\tilde{T}_\ell - \sum_{i=1}^N \mu_i}{\sqrt{\frac{\lambda}{2-\lambda}\sum_{i=1}^N \sum_{j=1}^N \mathrm{Cov}(Z_i^0, Z_j^0)}}\right) \qquad (15)$$

A. Performance Evaluation for Temporal LVDF

We examine next the performance of temporal LVDF in terms of target detection, using the approximation (15). The results shown are based on a network comprised of $N = 100$ sensors deployed on a grid, with the signal generated by model M1, the energy by $E_i^t = S_i + \epsilon_i^t$ and a stationary target located at the center of the region $\mathcal{R}$. Two scenarios are studied and compared: (1) Independent noise over time; i.e., $\mathrm{Cov}(\epsilon_i^t, \epsilon_i^{t-1}) = 0$, for all time slots t, with the noise $\epsilon_i^t \sim \mathcal{N}(0, \sigma^2)$ as before; (2) Temporally correlated noise according to the autoregressive model $\epsilon_i^t = \rho\epsilon_i^{t-1} + \xi_i$, with $\xi_i \sim \mathcal{N}(0, (1-\rho^2)\sigma^2)$, and $\epsilon_i^t \sim \mathcal{N}(0, \sigma^2)$ as before.

In Figure 9, ROC curves based on 1000 simulations for temporal LVDF under random deployment are shown for uncorrelated and correlated noise for time slots $t = \{0, 1, 2, 10\}$. The settings are $S_0 = 2$, $\eta = 0.1$, SNR $= 7$, $\alpha = 0.2$, $M = 9$, and $\lambda = 0.5$. As expected, for uncorrelated noise (left panel of Figure 9) the detection probability improves uniformly over time (given that the target is stationary) with gains of over 15% for small false alarm rates. More substantial gains are obtained for smaller targets (smaller values of η – results not shown here). It is interesting to note that most of the improvement occurs over the first two time slots, with rather minimal gains at subsequent times. Qualitatively, the situation is analogous if different weight factors λ are used, as well as in the case of square grid deployment.

For correlated noise, the ROC curves for time slot $t = 10$, under the above system settings and for values of $\rho = 0$ (uncorrelated noise), 0.4 and 0.9 are shown in the right panel of Figure 9. It can be seen that the performance degrades for larger values of the temporal correlation, a result which is consistent for other time slots as well. Nevertheless, for moderate values of ρ, the decrease in the detection probability is rather small, especially for smaller false alarm rates; this suggests that the procedure is fairly robust and hence useful in practice for weak temporal dependence scenarios.

We examine next the performance of temporal LVDF for different values of the weight parameter λ for moving targets across the monitored region R. Specifically, a target crosses R horizontally moving west to east, with the target's signal generated as before, over a monitoring period of 30 time units. The target appears at $t = 10$ and two scenarios for the target's speed are considered: in the first one, the target moves one hop every time unit and it takes 10 time periods to cross R; in the second scenario, the target moves 3 hops per time unit and it takes 3 time periods to cross R. The detection probability over the monitoring period for these two scenarios and for different values of λ is shown in Figure 10. It can be seen that for both slow (left panel) and fast (right panel) moving targets, the pattern is similar across λ: the detection probability rises fast once the target appears, stabilizes during its presence in R and fades once the target departs. The increase in the detection probability is similar for most values of λ with the exception of $\lambda = 0.2$, where a small lag is observed. On the other hand, there are substantial differences once the target departs; for example, for $\lambda = 0.2$ the detection probability fades slowly, since most of the weight is placed on past decisions, while for $\lambda = 1$ where all the weight is on the current decision, it drops to the false alarm rate almost immediately. We conclude that the intermediate value of $\lambda = 0.5$ is a reasonable and robust choice for most situations, since it is sensitive to both the emergence and departure of the target, and achieves a very high detection probability.

Remark: Under additional assumptions, the scenario involving a moving target could be formulated as a change-point problem.This formulation has been studied extensively, and optimal procedures and alternatives to EWMA can be derived as in, e.g., [20], [21], [22].

V. Discussion and Concluding Remarks

In this paper, we have proposed a new algorithm for decision fusion for target detection purposes, and the necessary decision threshold obtained through an analytical approximation of the system-wide false alarm probability, using limit theorems for weakly dependent random fields. The algorithm makes no assumptions about the signal model. Numerical results based on two models for signal attenuation show that the proposed

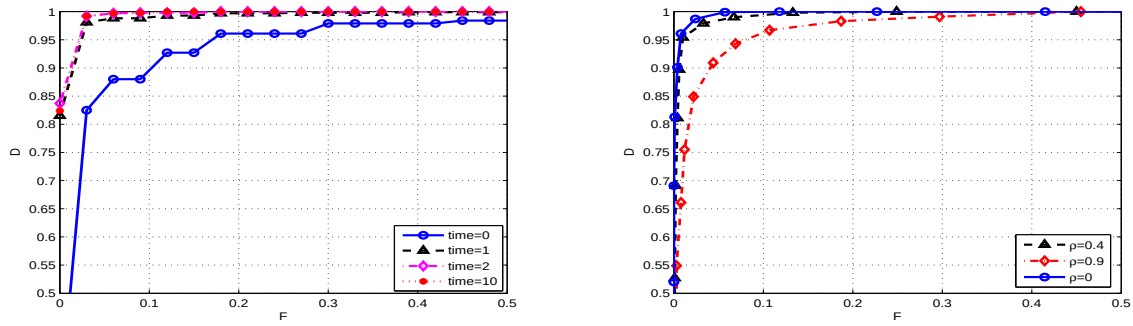

Fig. 9. Temporal LVDF probability of detection for different time slots and uncorrelated noise (left panel), and for a fixed time slot with different values of the correlation coefficient for correlated noise (right panel).

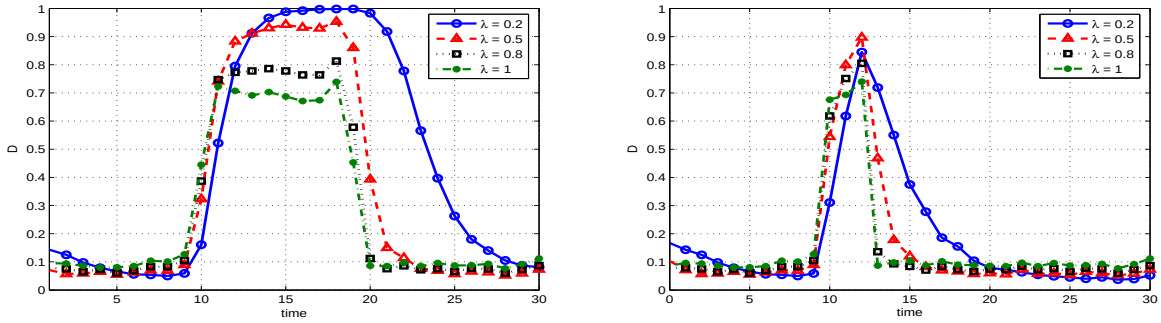

Fig. 10. Temporal LVDF probability of detection for slow (left panel) and fast moving targets (right panel) under a grid deployment.

scheme achieves significantly higher detection rates under a variety of settings, including sensor deployment mechanisms, signal strength, target size, etc. An extension to temporal decision fusion is also studied, and its performance assessed under different noise models and for moving targets. The new algorithm may prove useful for problems beyond target detection, e.g. localization and signal estimation; these are currently under investigation.

VI. Appendix

Here we establish the central limit theorem for correlated LVDF decisions Z_i which was used as the basis for the approximation (8). The key property of the variables Z_i we use here is that even though they are correlated, correlations are only present between 'nearby' locations.

Regular grids. The concept of correlations between 'nearby' locations is formalized in the notion of mixing. Let $\{X_i,\ i \in \mathbb{Z}^d\}$, $d \geq 1$, be a real-valued random field, i.e., a set of random variables defined on a d-dimensional lattice (in the present context $d = 2$). For any set of indices $E \subset \mathbb{Z}^d$, let $\mathcal{F}(X_E) = \mathcal{F}\{X_i;\ i \in E\}$ be the σ-field generated by the collection $\{X_i :\ i \in E\}$. Informally, $\mathcal{F}(X_E)$ contains all events related to the variables $\{X_i :\ i \in E\}$. Define $\alpha_{u,v}(k) = \sup\{|P(A \cap B) - P(A)P(B)| :\ A \in \mathcal{F}(X_E),\ B \in \mathcal{F}(X_F),\ |E| \leq u, |F| \leq v,\ \text{dist}(E,F) \geq k\}$, where the distance between two sets of indices E, F is defined as $\text{dist}(E,F) = \max\{\|x - y\|,\ x \in E, y \in F\}$, $\|x-y\| = \max_{j=1,\ldots,d} |x_j - y_j|$. Then the field $\{X_i\}$ is called α-mixing if for all u and v, $\alpha_{u,v}(k) \to 0$ as $k \to 0$.

The theory of mixing random fields has been studied extensively [23], [24]. We rely on the following theorem to establish the result.

Theorem 1: ([24], p.111). Let $X = \{X_i,\ i \in \mathbb{Z}^d\}$ be a real-valued field with $EX_i = 0$ (not necessarily stationary) and $\{D_n\}$ a sequence of strictly increasing finite domains of $\mathbb{Z}^d$. Let $S_n = \sum_{i \in D_n} X_i$ and let $\sigma_n^2 = \text{Var}(S_n)$. Assume that

(i) $\sum_{k=1}^{\infty} k^{d-1} \alpha_{u,v}(k) < \infty$, if $u+v \leq 4$ and $\alpha_{1,\infty}(k) = o(k^{-d})$.

(ii) There exists $\delta > 0$ such that $\sup_i ||X_i||_{2+\delta} < \infty$, and $\sum_{k=1}^{\infty} k^{d-1} \alpha_{1,1}(k)^{\frac{\delta}{2+\delta}} < \infty$.

(iii) $\liminf_n |D_n|^{-1} \sigma_n^2 > 0$.

Then,

$$\sigma_n^{-1} S_n \stackrel{\mathcal{D}}{\Rightarrow} \mathcal{N}(0,1). \tag{16}$$

Theorem 2: Let $\{Z_i,\ i = 1, \ldots, N\}$ be the LVDF corrected decisions on a regular grid with N nodes over the unit square, $D_N = (\frac{1}{\sqrt{N}}[1 : \sqrt{N}])^2$. Let $\mu_i = E(Z_i)$ and $S_N = \sum_{i=1}^{N} Z_i$. Then, as $N \to \infty$,

$$\frac{S_N - \sum_{i=1}^{N} \mu_i}{\sqrt{\text{Var}(S_N)}} \stackrel{\mathcal{D}}{\Rightarrow} \mathcal{N}(0,1). \tag{17}$$

The theorem holds for both D-LVDF and NN-LVDF.

Proof: The proof is carried out in two steps. The result is established first for the variables Z_i defined on a rescaled version of D_N, $\tilde{D}_N = ND_N = [1 : \sqrt{N}]^2$. Subsequently, it is extended to the original domain D_N.

The definition of the neighborhoods $U(i)$ (either circles of fixed radius as in D-LVDF, or M nearest neighbors as in NN-

LVDF) implies that the mixing coefficients $\alpha_{u,v}(k) \equiv 0$ for all $k \geq k_0$, with k_0 a fixed constant independent of N. Hence, all the conditions on the mixing coefficients in (i) and (ii) are automatically satisfied. Further, Z_i are binary and thus $||Z_i||_{2+\delta} \leq 1$ for all i and δ, which implies that condition (ii) holds as well.

Next, we establish condition (iii) holds in the present setting. Note that for all i and j, $P(Z_i = 1|Z_j = 1) \geq P(Z_i = 1)$, with strict inequality if $n_{ij} > 0$ and equality if $n_{ij} = 0$. Thus,

$$\text{Cov}(Z_i, Z_j) = [P(Z_i = 1|Z_j = 1) - P(Z_i = 1)]P(Z_j = 1) \geq 0.$$

Hence for $\sigma_N^2 \equiv \text{Var}(S_N) = \sum_{i,j} \text{Cov}(Z_i, Z_j)$ we have

$$\sigma_N^2 \geq \sum_{i=1}^{N} \text{Var}(Z_i) \geq N \inf_i \sigma_i^2 = N\sigma_0^2. \tag{18}$$

For the fixed number of neighbors case, we have $\mu_i = \mu = \sum_{j=[M/2]+1}^{M} \binom{M}{j} \alpha^j (1-\alpha)^{M-j}$ and $0 < \mu < 1$. For the fixed radius case on a regular grid, the only possible values for M_i are in the set $\{1, \ldots, M\}$, where M is the full neighborhood size (unaffected by edges). Hence, there is a finite, at most M, number of μ_i and for each one $0 < \mu_i < 1$, so that $\sigma_0^2 = \inf_i \mu_i(1-\mu_i) > 0$, which in turn implies that $\lim_{N\to\infty} |\tilde{D}_N|^{-1} \sigma_N^2 = \lim_{N\to\infty} N^{-1}\sigma_N^2 > 0$.

On the original domain D_N (grid over the unit square), consider first the case of M nearest neighbors. The joint distribution of the $\{Z_i\}$s over D_N is identical to that over $\tilde{D}_N$ for each N, which shows that the same limit (17) holds. For the fixed radius neighborhood case, in order to make the joint distribution of the $\{Z_i\}$s invariant to rescaling of the grid, select $r = r_N \to 0$ so that $r_N = O(\sqrt{N})$. A convenient choice is to set $N\pi r_N^2 = M = \text{const}$ as before, thus fixing the size of the neighborhoods not adjacent to the edges of the unit square. Then, the limit (17) holds for D-LVDF as well.

Random deployments. For the case of random deployments, we need a central limit theorem for a functional $H(\mathcal{X})$ of a marked binomial point process $\mathcal{X} = \{X_i = (s_i, d_i), i = 1, \ldots, N\}$, where s_i are the random sensor locations and d_i are the original i.i.d. decisions (the marks). A general CLT for unmarked binomial and Poisson processes was obtained in [25] and extended to marked point processes in [26]. The functional H must be translation-invariant and satisfy two conditions:

(i) H is *strongly stabilizing*, which, informally speaking, means that the "add one cost" $\Delta(\mathcal{X}) = H(\mathcal{X} \cup \{0\}) - H(\mathcal{X})$, i.e., the change in H caused by inserting an extra point at the origin, is not affected by changes in $\mathcal{X}$ that are far from the origin; and

(ii) Certain moment bounds hold for $\Delta(\mathcal{X})$ and $H(\mathcal{X})$.

For lack of space, we do not state or check these conditions formally, but they are easy to verify for LVDF: (i) is implied by the neighborhood structure, and (ii) follows from the fact that all the variables are binary. Rescaling to the unit square from an increasing domain is done in the same way as for regular grids.

REFERENCES

[1] J. Elson and D. Estrin, *Sensor Networks: a Bridge to the Physical World*. Kluwer Academic Publishers, Norwell, MA, USA, 2004.

[2] T. Clouqueur, V. Phipatanasuphorn, K. Saluja, and P. Ramanathan, "Sensor deployment strategy for detection of targets traversing a region," *Mobile Networks and Applications*, vol. 28, no. 8, pp. 453–461, 2003.

[3] R. Viswanathan and P. Varshney, "Distributed detection with multiple sensors: Part I-Fundamentals," *Proc. IEEE*, vol. 85, no. 1, pp. 54–63, January 1997.

[4] R. Tenney and N. Sandell, "Detection with distributed sensors," *IEEE Trans. Aerosp. Electron. Syst.*, vol. 17, no. 3, pp. 501–510, 1981.

[5] Z. Chair and P. Varshney, "Optimal data fusion in multiple sensor detection systems," *IEEE Trans. Aerosp. Electron. Syst.*, vol. 22, no. 1, pp. 98–101, 1986.

[6] M. Kam, Q. Zhu, and W. Gray, "Optimal data fusion of correlated local decisions in multiple sensor detection systems," *IEEE Trans. Aerosp. Electron. Syst.*, vol. 28, no. 3, pp. 916–920, 1992.

[7] Y. Sung, L. Tong, and A. Swami, "Asymptotic locally optimal detector for large scale sensor network under the poisson regime," *IEEE Trans. Signal Processing*, vol. 53, no. 6, pp. 2005–2017, June 2005.

[8] B. Chen and P. Varshney, "A Bayesian sampling approach to decision fusion using hierarchical models," *IEEE Trans. on Signal Processing*, vol. 50, no. 8, pp. 1809–1818, August 2002.

[9] R. Niu, B. Chen, and P. Varshney, "Fusion of decisions transmitted over Rayleigh fading channels in wireless sensor networks," *IEEE Trans. Signal Processing*, vol. 54, no. 3, pp. 1018–1027, March 2006.

[10] R. Niu and P. Varshney, "Performance evaluation of decision fusion in wireless sensor networks," in *Proc. 40th Annual Conf. Info. Sciences Systems*, March 2006.

[11] R. Niu, P. Varshney, and Q. Cheng, "Distributed Bayesian algorithms for fault-tolerant event region detection in wireless sensor networks," *Intl. Journal on Information Fusion*, vol. 53, 2004.

[12] S. Aldosari and J. Moura, "Saddlepoint approximation for sensor network optimization," in *Proc. IEEE Int. Conf. on Acoustics, Speech, and Signal Processing (ICASSP'05)*, vol. 4, March 2005, pp. iv/741–iv/744.

[13] M. Zhu, S. Ding, R. Brooks, Q. Wu, N. Rao, and S. Lyengar, "Fusion of threshold rules for target detection in sensor networks," *ACM Transactions on Sensors Networks*, 2005, submitted.

[14] M. Duarte and Y. Hu, "Distance-based decision fusion in a distributed wireless sensor network," *Telecommunication Systems*, vol. 26, no. 2-4, pp. 339–350, June 2004.

[15] T. Sun, L. Chen, C. Han, and M. Gerla, "Reliable sensor networks for planet exploration," in *Proc. IEEE Intl. Conf. Networking, Sensing and Control*, 2005.

[16] L. Klein, "A Boolean algebra approach to multiple sensor voting fusion," *IEEE Trans. Aerosp. Electron. Syst.*, vol. 29, no. 2, pp. 317–327, April 1993.

[17] A. Tartakovsky and V. Veeravalli, "Quickest change detection in distributed sensor systems," in *Proc. 6th Int. Conf. on Information Fusion, Cairns, Australia*, July 2003, pp. 756–763.

[18] D. Li, K. Wong, Y. Hu, and A. Sayeed, "Detection, classification, and tracking of targets," *IEEE Signal Processing Magazine*, vol. 19, no. 2, pp. 17–29, 2002.

[19] T. Clouqueur, P. Ramanathan, K. Saluja, and K. Wang, "Value-fusion versus decision-fusion for fault-tolerance in collaborative target detection in sensor networks," in *Proc. 4th Ann. Conf. on Information Fusion*, 2001, pp. TuC2/25–TuC2/30.

[20] A. Tartakovsky and V. Veeravalli, "Change point detection in multichannel and distributed systems with applications," *Applications of Sequential Methodologies*, pp. 339–370, 2004.

[21] A. Tartakovsky and H. Kim, "Performance of certain decentralized distributed change detection procedures," in *Proc. 9th Int. Conf. on Information Fusion, Florence, Italy*, ser. IEEE Catalog No. 06EX1311C, July 2006.

[22] A. Tartakovsky, B. Rozovskii, R. Blaŷzek, and H. Kim, "Detection of intrusions in information systems by sequential change-point methods (with discussion)," *Statistical Methodology*, vol. 3, pp. 252–340, 2006.

[23] P. Doukhan, *Mixing: Properties and Examples*. Springer–Verlag, 1994.

[24] X. Guyon, *Random Fields on a Network: Modeling, Statistics, and Applications*. Springer–Verlag, New York, 1995.

[25] M. Penrose and J. Yukich, "Central limit theorems for some graphs in computational geometry," *Ann. Appl. Prob.*, vol. 11, pp. 1005–1041, 2001.

[26] ——, "Limit theory for random sequential packing and deposition," *Ann. Appl. Prob.*, vol. 12, pp. 272–301, 2002.